International Journal of Nanoelectronics and Materials
IJNeaM
ISSN 1985-5761 | E-ISSN 2232-1535

Microwave plasma-enhanced chemical vapor deposition growth of graphene nanowalls on varied substrates: A comparative study

Rucheng Zhu [a,b] *, Riteshkumar Vishwakarma [a], Haibin Li [b], DeQuan Yao [c], Masayoshi Umeno [a], and Tetsuo Soga [b] *

[a]*C's Techno Inc., Co-operative Research Center for Advanced Technology, Nagoya Science Park, Moriyama-ku, Nagoya Aichi 4630018, Japan*
[b]*Department of Electrical and Mechanical Engineering, Nagoya Institute of Technology, Gokiso-cho, Showa-ku, Nagoya Aichi 466-8555, Japan*
[c]*Santec Holdings Corporation 5823 Ohkusa-Nenjozaka, Komaki, Aichi 485-0802, Japan*
** Corresponding author. Tel.: +81-52-735-5532; fax: +81-52-735-7120; e-mail: soga@nitech.ac.jp, r.zhu.433@stn.nitech.ac.jp*

Received 18 July 2024, Revised 29 August 2024, Accepted 14 October 2024

ABSTRACT

We explored the growth rate and morphological characteristics of graphene nanowalls (GNWs) on copper (Cu), stainless steel (SUS), quartz and silicon (Si) substrates by changing the growth time using microwave plasma-enhanced chemical vapor deposition (MWPCVD). Furthermore, we investigated the impact of catalytic and non-catalytic substrates on the growth features of GNWs. The properties of GNWs were characterized using scanning electron microscopy (SEM) and Raman spectroscopy. The growth of GNWs occurred just after supplying the precursor on the Cu substrate, but those on SUS, quartz and Si delayed about 5 min, 10 min and 15 min, respectively, due to the low catalytic activity of the substrate. Once the growth started, there was not much of a difference in the growth rate. The average growth rate was about 2 nm/s. The crystallinity of GNW was improved with increasing growth time. It was found that Cu is the best substrate to get high-quality GNWs, but MWPCVD is a suitable technique to obtain GNWs on a variety of substrates at relatively low temperatures.

Keywords: *Graphene, Graphene nanowall, MWPCVD, Growth rate, Catalyst, Raman, SEM*

1. INTRODUCTION

The discovery of graphene has accelerated the rapid development of nanotechnology. Carbon-based materials have various applications and promising prospects due to their unique range of physical and chemical properties [1-4]. For instance, zero-dimensional structures such as fullerenes [5], one-dimensional structures like carbon nanotubes (CNT) and carbon nanofibers (CNF) [6], two-dimensional materials including single-layer graphene and multilayer graphene [7], and carbon nanoribbons (GNR) [8], as well as three-dimensional structures like graphene nanowalls [9-11]. Compared with two-dimensional graphene synthesized by conventional chemical processes, three-dimensional graphene networks produced by plasma CVD show many unique features, such as vertical orientation on the substrate, non-agglomerated three-dimensional morphology, and controlled inter-sheet connectivity. These structural characteristics render GNWs with excellent electrical and thermal conductivity, high specific surface area, high chemical stability, outstanding mechanical strength and flexibility, and tunable optical properties [12-15]. Furthermore, GNWs have garnered significant attention in various fields, including supercapacitors, batteries, fuel cells, etc [16-22].

The synthesis of GNWs is mainly accomplished with MWPCVD [23-28]. This method allows for direct growth on various substrates, including insulators, semiconductors, and conductors. The presence of materials like copper and nickel acts as catalysts for graphene growth, significantly affecting the initial growth time, surface morphology, crystallinity, and electronic properties of GNWs on different substrates. Furthermore, differences in equipment and deposition conditions can lead to variations in GNWs growth rates and morphologies. Therefore, to investigate the substrate effect on GNW growth is very important to understand the GNW growth mechanisms on various substrates. Davami et al reported a comparison of GNW growth using Cu, Si and Si covered with metal using RF plasma-enhanced chemical vapor deposition [29]. Kim et al reported the difference in GNWs on glass and Si substrates [30]. However, to the best of our knowledge, there have been no systematic studies of GNW growth on the growth rates and morphologies on metal, insulating and semiconducting Si substrates prepared using the MWPCVD method.

In this study, we employed the MWPCVD method to directly grow GNWs on Cu foils, SUS foils, quartz, and highly doped n-type silicon (Si with a resistivity of 1Ω·cm) substrates. We observed the impact of these substrates on GNWs growth. The surface morphology and crystallinity of the obtained GNWs were characterized using scanning electron microscopy (SEM) and Raman spectroscopy. The results demonstrated a linear relationship between the growth height and time for GNWs on metal substrates like Cu and SUS. The ability to achieve rapid GNWs growth on catalytic

substrates opens the possibility of high-speed production of GNWs films.

2. METHODOLOGY

The MWPCVD equipment used in this study is the same as reported previously [31] and illustrated in Figure 1. In brief, it consists of a magnetron (2.45 GHz microwave radiation), waveguide which guides the microwave radiation to the quartz plate, slot antenna which filters out unwanted harmonics and delivers the 2.45 GHz microwave radiation to the quartz plate, coupling adjustment knob which adjusts the wave shape within the waveguide to ensure smooth transmission of microwaves through the slot antenna, quartz plate which allows the microwave radiation to enter from its surface and gas inlet port which is used for introducing precursor and carrier gases into the reaction chamber.

All the samples of GNWs were prepared under the identical growth conditions of microwave plasma power 1000 W, with the source and carrier gas flow rate of CH_4:H_2:Ar = 3:8:8 sccm maintaining a working chamber pressure of 10 Pa. The stage temperature was set at 500 ^oC and all the gases purged were of research grade of 99.999% purity. The growth duration varied from 5, 10, 15 and 20 minutes on the four types of distinct substrates: quartz as an insulating substrate, n-type silicon as a semiconducting substrate, Cu as a metallic catalytic substrate and SUS304 as an alloy substrate. The SEM characterization was performed to evaluate the surface morphology and thickness of the films using JEOL Ltd. JIB-4700F FIB-SEM. The transmission electron microscopy (TEM) characterization was performed to evaluate the thickness of graphene using JEOL Ltd. JEM-2100F. Raman spectroscopy was performed to evaluate the structural properties using Renishaw InVia

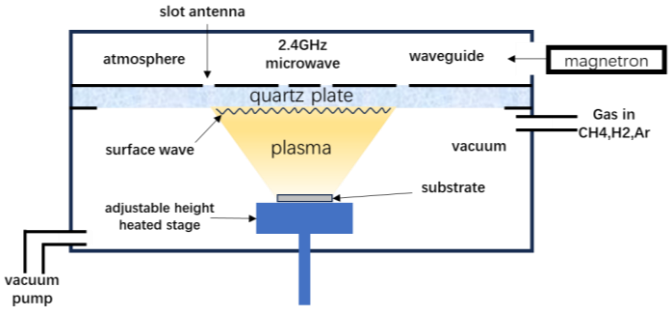

Figure 1. Schematic of the MWPCVD equipment

Laser Raman spectroscope with an excitation laser wavelength of 532 nm.

3. RESULTS AND DISCUSSION

3.1. SEM and TEM Analysis

Figure 2 shows surface SEM images of GNWs on Cu, SUS, quartz and Si substrates for different growth times; 5 min, 10 min, 15 min and 20 min. "-" in the figure means GNW has not started to grow yet. GNWs have already started to grow within the first 5 minutes in the case of Cu substrate. The height of GNWs increases linearly with the growth time as shown in Figure 3. The size of GNW also increases with increasing growth time. The growth rate is approximately 2 nm/s. Since the Cu substrate has a catalytic effect on graphene growth [32], crystallization begins promptly after the growth starts. Under the same experimental conditions, carbon-free radicals deposit at the same rate in the vertical direction, resulting in a linear growth rate for GNWs. However, due to the presence of H^+ and CH_x^+ ions in the plasma, there is an etching effect, and the growth rate in the horizontal direction is slower than in the vertical direction.

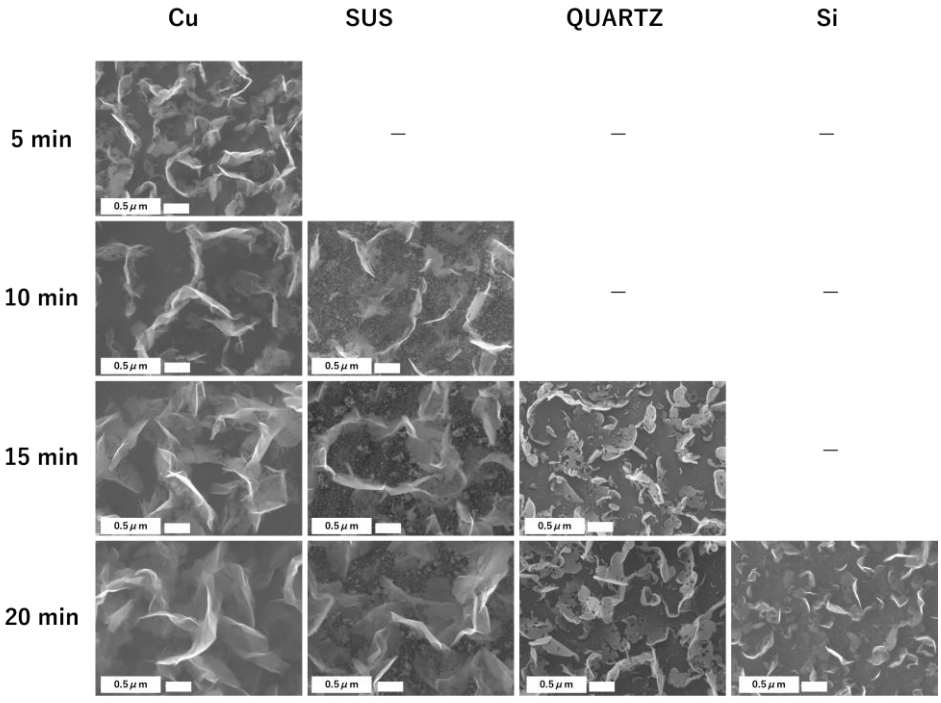

Figure 2. SEM surface images of GNWs on different substrates for various growth times

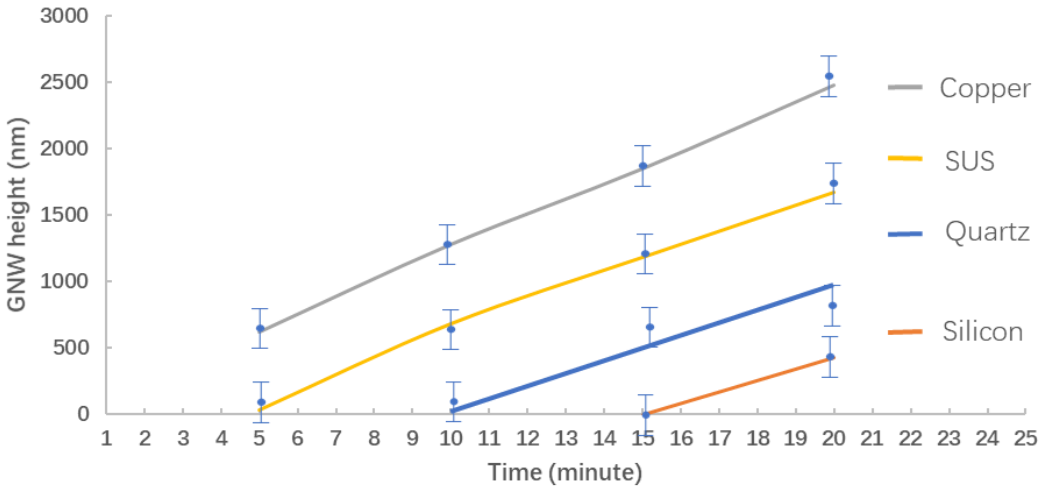

Figure 3. GNW average height for different growth times on four substrates

On the other hand, GNWs have not started to grow yet in the first 5 min in the case of SUS substrate and GNWs are observed after 10 min. The composition analysis of SUS304 reveals that, apart from iron (Fe), it contains approximately 20% chromium (Cr), 10% nickel (Ni), 2% manganese (Mn), and other metals. Nickel is known to have a better catalytic effect on graphene growth [33]. However, since the nickel content in SUS304 is only 8-10%, its growth-promoting effect is not as pronounced as that of copper substrates. Therefore, graphene growth does not commence in the initial 5 minutes. But once growth starts, the growth height of GNWs begins to show a linear relationship with time during the 10-20 min period and the growth rate is almost the same as that on Cu as shown in Figure 3. Thus, unlike the pure Cu substrate, the SUS substrate with a limited Ni content provides a controlled catalytic activity for the growth of GNWs almost at the same rate as that of Cu.

It is interesting to note that the growth of GNWs is further delayed in the case of quartz substrate. In the samples of 5- and 10-min growth time, no GNW was observed, but we observed uniform growth of GNWs after 15 min. The height of GNWs increases with time after the growth initiation as shown in Figure 3. This suggests that carbon atoms deposited on the substrate surface in the first 10 minutes of the experiment did not crystallize. This might be because during plasma-enhanced deposition, the etching effect of H+ was greater than the deposition effect, preventing accumulation. However, after 10 min, as the number of carbon atoms in the chamber increased, the deposition effect exceeded the etching effect, resulting in crystallization. With increasing time, GNWs began to grow in a direction perpendicular to the substrate and with a higher plasma concentration above the substrate.

In the case of the Si substrate, no GNW was detected for 5, 10, and 15 minutes, but we can see that GNWs have begun to grow after 20 minutes as shown in Figure 3. The height of GNWs is slightly lower than that on the quartz glass substrate. The GNWs grown on the Si substrate took the longest time. Like quartz glass, the silicon substrate lacks a catalytic effect on the crystalline growth of graphene. However, due to silicon's higher crystallinity and fewer polished surface defects, carbon-free radicals have weaker adhesion during deposition. Under the same plasma concentration conditions, the deposition effect is less pronounced, requiring more time to reach an equivalent rate as the etching effect. When the deposition rate exceeds the etching rate, GNWs with a morphology similar to those on quartz glass also grow on the silicon substrate.

The GNW was evaluated by TEM to check the thickness of the graphene flake. To prepare the TEM sample, the GNW grown on the SUS304 substrate was obtained in the powdered form, sonicated in ethanol and drop cast on a TEM grid with pipette. The high magnification TEM image shown in Figure 4 clearly reveals the array of graphene layers in a leaflet of GNW, aggregating a thickness of about 15 nm.

3.2. Raman Spectroscopy Analysis

To gain insights into the structural properties of GNWs, Raman spectroscopy analysis was performed. Figure 5

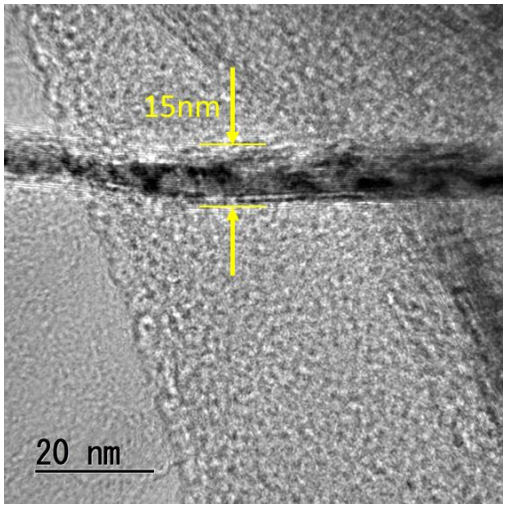

Figure 4. TEM image of GNW grown on SUS substrate

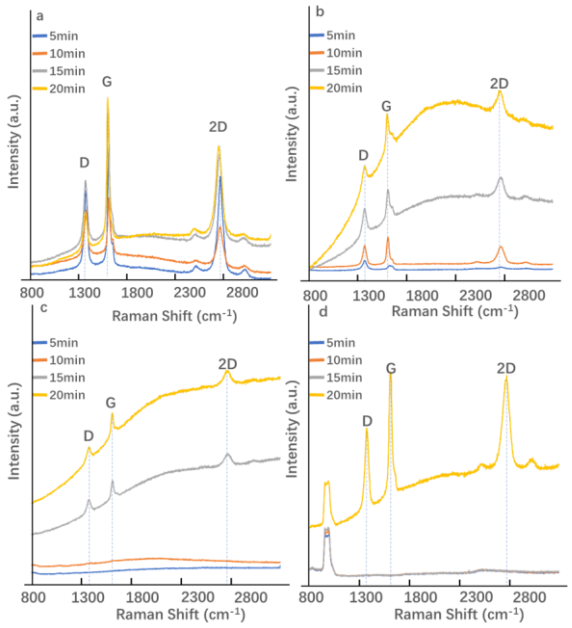

Figure 5. Raman spectra achieved on the GNWs with different growth times on (a) Cu, (b) SUS, (c) quartz and (d) Si substrates

presents Raman spectra of GNWs grown on various substrates at different deposition times. Figure 5(a) corresponds to the copper substrate, (b) to the SUS substrate, (c) to a quartz glass substrate and (d) to the Si substrate. It is evident that under the same deposition conditions, GNWs exhibit different initial nucleation times. Characteristic peaks of graphene are detected on Cu substrate after 5 min growth, while the corresponding peaks appear after 10 min, 15 min and 20 min on SUS substrate, quartz substrate and Si substrate, respectively. The broad peak from the 5-minute sample on SUS would be due to the amorphous carbon deposited on the SUS substrate. This observation matches with SEM results as shown in Figure 2 and suggests that the growth of GNWs on glass and n-type Si substrates requires a longer time under equivalent conditions. These Raman spectroscopy observations provide valuable information about the growth processes of GNWs on different substrates and the development of crystalline structures over time.

The Raman spectra of GNWs grown on different substrates exhibited characteristic peaks around 1350 cm^{-1} (D band), 1580 cm^{-1} (G band), and 2700 cm^{-1} (2D band). The D band originates from defects in the graphene lattice, while the G band is related to the in-plane vibrational modes of sp2 hybridized carbon atoms [26-28]. The 2D band represents the number of graphene layers and the quality of graphene [28]. Moreover, the distinct peak at the shoulder to the G band centered around 1620 cm^{-1} is a characteristic feature of the vertical graphene [34]. The intensity ratio of the D band to the G band (I_D/I_G) is an important parameter reflecting the level of disorder and defects in the graphene lattice. A higher I_D/I_G ratio indicates a higher degree of disorder. The intensity ratio of the 2D band to the G band (I_{2D}/I_G) reveals the thickness of the graphene. The Raman spectra of GNWs grown on different substrates show minor variations in the intensity and position of the D and G bands, indicating structural and electronic property differences in GNWs [35-37].

Table 1 depicts the changes in I_D/I_G and I_{2D}/I_G obtained from Raman spectra of GNWs grown on Cu, SUS, quartz and Si substrates. The measured values of I_D/I_G are 0.60, 0.81, 0.48, and 0.21 at 5 min, 10 min, 15 min and 20 min, respectively, for Cu substrate. This trend of initially increasing and then decreasing I_D/I_G suggests the rapid formation of graphene films on the Cu surface at the initial stages of the growth. After 10 min growth, graphene growth exhibited a distinct trend of vertical crystal growth, accompanied by the generation of many defects and amorphous structures. Therefore, an increase in I_D/I_G is observed. As time progresses, I_D/I_G gradually decreases, indicating the improvement in crystallinity of vertically oriented graphene with the increase of thickness [24, 30-31]. The increase of I_{2D}/I_G would be due to the increase of layer number with the growth time.

In the case of the SUS substrate, I_D/I_G is high because of the deposition of amorphous carbon at 5 min. However, like the Cu substrate, the increase and the decrease of I_D/I_G as well as the decrease of I_{2D}/I_G are observed with the growth time in the case of SUS substrate. However, the variation of the intensity is less compared with the Cu substrate. In the case of the quartz substrate, I_D/I_G and I_{2D}/I_G decrease, which suggests the improvement of crystallinity and increase of layer number with growth time.

Simultaneously, we observed the shifting of G and 2D peaks with increasing deposition time on the Cu substrate. Consequently, we have zoomed in on the Raman spectroscopy data of the G and 2D peaks for four different samples on the Cu substrate, as depicted in Figure 6.

Figure 6 indicates that peak wavelength shifts towards the lower wavenumber side for the G peak and 2D peak. The shifting of graphitic G and 2D peaks is in good agreement

Table 1. Raman I_D/I_G and I_{2D}/I_G values of GNWs on each substrate at different growth times

	Cu		SUS304		Quartz		Silicon	
Growth Time	I_D/I_G	I_{2D}/I_G	I_D/I_G	I_{2D}/I_G	I_D/I_G	I_{2D}/I_G	I_D/I_G	I_{2D}/I_G
5min	0.60	0.77	2.28	0.43	---	---	---	---
10min	0.81	0.71	0.72	0.61	---	---	---	---
15min	0.48	0.65	0.88	0.63	0.70	0.61	---	---
20min	0.21	0.62	0.58	0.57	0.60	0.58	0.66	0.72

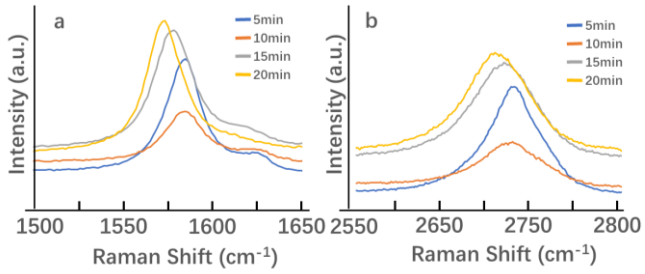

Figure 6. Shifting of G and 2D peak positions of Raman spectra of GNWs on Cu substrate with different growth times

with research reported elsewhere. As the growth time increases, the thickness of the film also increases, as does the number of layers [32, 34, 38]. The results indicate that the growth process involves an initial rapid formation of graphene, followed by the formation of vertically orientated graphene with increasing deposition time, simultaneously leading to an improvement in crystallinity and thickness, which is consistent with the I_D/I_G and I_{2D}/I_G results. These experimental observations provide new insights into the mechanism of graphene growth on Cu substrates. However, this displacement phenomenon was not obviously observed in the GNW samples grown on SUS304 substrate. The variation of I_D/I_G and I_{2D}/I_G is also small, as shown in Table 1. These experimental observations provide new insights into the mechanism of graphene growth on copper substrates.

3.3. Discussion

As shown in Figure 3, the growth height of GNWs on Cu, SUS and quarts substrates exhibits a fundamentally linear relationship. Additionally, the incubation times for GNW growth vary significantly across the four types of substrates. Therefore, we believe that under plasma irradiation conditions, carbon can be deposited on different substrates, producing GNWs. However, due to variations in the composition of different substrates, the initial growth time varies. This is mainly because carbon elements deposited on Cu substrate with catalytic properties crystallize under the catalytic effect of copper, forming growth nuclei. Graphene starts growing in all directions around these growth nuclei. However, as the plasma concentration gradually decreases from the quartz glass towards the stage direction, GNWs growth tendency is most prominent in the vertical direction of the substrate, while horizontal growth of graphene is suppressed due to the etching effect of H^+ ions in the plasma.

When GNWs grow on SUS substrate, the growth time is delayed compared to Cu substrate because only nickel in SUS has catalytic properties for graphene growth, and the nickel content in SUS is only about 10%. Additionally, iron also exhibits some catalytic activity during graphene growth. After the initial growth begins, the growth rate of GNWs on the SUS substrate becomes quite similar to that on the Cu substrate.

For substrates like quartz and silicon, which lack graphene catalytic activity, carbon deposition on these substrates is slower, and even in samples from the first more than 10 minutes, crystalline carbon is not detected. As time progresses, carbon deposited on the substrate gradually increases, and crystallization begins. GNWs grown on these substrates appear relatively smaller in volume and have larger distances between crystals. This is primarily due to the simultaneous etching effect of H^+ ions and the weak growth of GNWs. Extended growth times are required to achieve normal growth [39].

4. CONCLUSION

CNWs were grown on Cu, SUS, quartz and Si substrates under the same conditions with changing the growth time by MWPCVD. The MWPCVD method allows for the direct synthesis of CNWs on various substrates using methane as a precursor gas. However, the catalytic effects were different depending on substrates, such as Cu and SUS with catalytic properties and quartz glass and Si without catalytic properties, which results in variations in the growth rate and morphology of GNWs. Therefore, the choice of substrate is crucial when synthesizing GNWs by MVPCVD for different applications.

REFERENCES

[1] A. K. Geim and K. S. Novoselov, “The rise of graphene,” *Nature Materials*, vol. 6, no. 3, pp. 183–191, 2007.
[2] A. K. Geim, “Graphene: Status and Prospects,” *Science*, vol. 324, no. 5934, pp. 1530–1534, 2009.
[3] A. H. Castro Neto, F. Guinea, N. M. R. Peres, K. S. Novoselov, and A. K. Geim, “The electronic properties of graphene,” *Reviews of Modern Physics*, vol. 81, no. 1, pp. 109–162, 2009.
[4] A. A. Balandin, “Thermal properties of graphene and nanostructured carbon materials,” *Nature Materials*, vol. 10, no. 8, pp. 569–581, 2011.
[5] M. Prato, “Fullerene Materials,” 1999, pp. 173–187.
[6] B. M. Tyson, R. K. Abu Al-Rub, A. Yazdanbakhsh, and Z. Grasley, “Carbon Nanotubes and Carbon Nanofibers for Enhancing the Mechanical Properties of Nanocomposite Cementitious Materials,” *Journal of Materials in Civil Engineering*, vol. 23, no. 7, pp. 1028–1035, 2011.
[7] J. Phiri, P. Gane, and T. C. Maloney, “General overview of graphene: Production, properties and application in polymer composites,” *Materials Science and Engineering: B*, vol. 215, pp. 9–28, 2017.
[8] L. Jiao, L. Zhang, L. Ding, J. Liu, and H. Dai, “Aligned graphene nanoribbons and crossbars from unzipped carbon nanotubes,” *Nano Research*, vol. 3, no. 6, pp. 387–394, 2010.
[9] S. R. Waite and S. Nazarpour, “Graphene Technology: The Nanomaterials Road Ahead,” in *Graphene Technology: From Laboratory to Fabrication*, Weinheim, Germany: Wiley-VCH Verlag GmbH & Co. KGaA, 2016, pp. 1–17.
[10] H. J. Cho, H. Kondo, K. Ishikawa, M. Sekine, M. Hiramatsu, and M. Hori, “Density control of carbon nanowalls grown by CH4/H2 plasma and their electrical properties,” *Carbon*, vol. 68, pp. 380–388, 2014.

[11] L. Giorgi, T. Makris, R. Giorgi, N. Lisi, And E. Salernitano, "Electrochemical properties of carbon nanowalls synthesized by HF-CVD," *Sensors and Actuators B: Chemical*, vol. 126, no. 1, pp. 144–152, 2007.

[12] A. Jagodar *et al.*, "Growth of graphene nanowalls in low-temperature plasma: Experimental insight in initial growth and importance of wall conditioning," *Applied Surface Science*, vol. 643, p. 158716, 2024.

[13] H. Park, S. O. Jang, J.-H. Shin, K. il Lee, and Y. S. Choi, "Large-Scale Carbon Nanowall Synthesis Using Upgraded ReSLAN Plasma Source," *IEEE Transactions on Plasma Science*, vol. 52, no. 4, pp. 1174–1181, 2024.

[14] H. Watanabe, H. Kondo, M. Sekine, M. Hiramatsu, and M. Hori, "Control of Super Hydrophobic and Super Hydrophilic Surfaces of Carbon Nanowalls Using Atmospheric Pressure Plasma Treatments," *Japanese Journal of Applied Physics*, vol. 51, no. 1S, p. 01AJ07, 2012.

[15] H. Ci *et al.*, "6-inch uniform vertically-oriented graphene on soda-lime glass for photothermal applications," *Nano Research*, vol. 11, no. 6, pp. 3106–3115, 2018.

[16] N. Van Toan, H. Sui, J. Li, T. T. K. Tuoi, and T. Ono, "Nanoengineered micro-supercapacitors based on graphene nanowalls for self-powered wireless sensing system," *Journal of Energy Storage*, vol. 81, p. 110446, 2024.

[17] S. Ghodke *et al.*, "Mechanical properties of maze-like carbon nanowalls synthesized by the radial injection plasma enhanced chemical vapor deposition method," *Materials Science and Engineering: A*, vol. 862, p. 144428, 2023.

[18] Z. Bo *et al.*, "Vertically Oriented Graphene Bridging Active-Layer/Current-Collector Interface for Ultrahigh Rate Supercapacitors," *Advanced Materials*, vol. 25, no. 40, pp. 5799–5806, 2013.

[19] A. Reguig *et al.*, "Graphene nanowalls grown on copper mesh," *Nanotechnology*, vol. 35, no. 8, p. 085602, Feb. 2024.

[20] K. Yu, G. Lu, Z. Bo, S. Mao, and J. Chen, "Carbon Nanotube with Chemically Bonded Graphene Leaves for Electronic and Optoelectronic Applications," *The Journal of Physical Chemistry Letters*, vol. 2, no. 13, pp. 1556–1562, 2011.

[21] K. Kim, C. Kim, S. Kwon, W. Choi, and H. Kang, "Graphite Slurry Heat Treatment Temperature for Improving the Durability of CNWs Anode Materials of Lithium-Ion Batteries," *Journal of Electrical Engineering & Technology*, vol. 19, no. 1, pp. 791–797, 2024.

[22] M. Cai, R. A. Outlaw, S. M. Butler, and J. R. Miller, "A high density of vertically-oriented graphenes for use in electric double layer capacitors," *Carbon*, vol. 50, no. 15, pp. 5481–5488, 2012.

[23] J. Kulczyk-Malecka, I. V. J. dos Santos, M. Betbeder, S. J. Rowley-Neale, Z. Gao, and P. J. Kelly, "Low-temperature synthesis of vertically aligned graphene through microwave-assisted chemical vapour deposition," *Thin Solid Films*, vol. 733, p. 138801, 2021.

[24] M. Zeng, Y. Xiao, J. Liu, W. Lu, and L. Fu, "Controllable Fabrication of Nanostructured Graphene Towards Electronics," *Advanced Electronic Materials*, vol. 2, no. 4, 2016.

[25] M. Hiramatsu, K. Shiji, H. Amano, and M. Hori, "Fabrication of vertically aligned carbon nanowalls using capacitively coupled plasma-enhanced chemical vapor deposition assisted by hydrogen radical injection," *Applied Physics Letters*, vol. 84, no. 23, pp. 4708–4710, 2004.

[26] R. Liu, Y. Chi, L. Fang, Z. Tang, and X. Yi, "Synthesis of Carbon Nanowall by Plasma-Enhanced Chemical Vapor Deposition Method," *Journal of Nanoscience and Nanotechnology*, vol. 14, no. 2, pp. 1647–1657, 2014.

[27] M. Hiramatsu, K. Ito, C. H. Lau, J. S. Foord, and M. Hori, "Fabrication of vertically aligned carbon nanostructures by microwave plasma-enhanced chemical vapor deposition," *Diamond and Related Materials*, vol. 12, no. 3–7, pp. 786–789, 2003.

[28] K. Shiji, M. Hiramatsu, A. Enomoto, M. Nakamura, H. Amano, and M. Hori, "Vertical growth of carbon nanowalls using rf plasma-enhanced chemical vapor deposition," *Diamond and Related Materials*, vol. 14, no. 3–7, pp. 831–834, 2005.

[29] K. Davami *et al.*, "Synthesis and characterization of carbon nanowalls on different substrates by radio frequency plasma enhanced chemical vapor deposition," *Carbon*, vol. 72, pp. 372–380, 2014.

[30] S. Y. Kim, Y. H. Joung, and W. S. Choi, "Growth properties of carbon nanowalls on glass substrates by a microwave plasma-enhanced chemical vapor deposition," *Japanese Journal of Applied Physics*, vol. 53, no. 5S1, p. 05FD09, 2014.

[31] R. Vishwakarma *et al.*, "Direct Synthesis of Large-Area Graphene on Insulating Substrates at Low Temperature using Microwave Plasma CVD," *ACS Omega*, vol. 4, no. 6, pp. 11263–11270, 2019.

[32] A. Reguig *et al.*, "Graphene nanowalls grown on copper mesh," *Nanotechnology*, vol. 35, no. 8, p. 085602, 2024.

[33] K. S. Kim *et al.*, "Large-scale pattern growth of graphene films for stretchable transparent electrodes," *Nature*, vol. 457, no. 7230, pp. 706–710, 2009.

[34] A. Gupta, G. Chen, P. Joshi, S. Tadigadapa, and Eklund, "Raman Scattering from High-Frequency Phonons in Supported n -Graphene Layer Films," *Nano Letters*, vol. 6, no. 12, pp. 2667–2673, 2006.

[35] R. Vishwakarma *et al.*, "Fabrication of particular structures of hexagonal boron nitride and boron–carbon–nitrogen layers by anisotropic etching," *Physica E: Low-dimensional Systems and Nanostructures*, vol. 79, pp. 13–19, 2016.

[36] J. Zhao, M. Shaygan, J. Eckert, M. Meyyappan, and M. H. Rümmeli, "A Growth Mechanism for Free-Standing Vertical Graphene," *Nano Letters*, vol. 14, no. 6, pp. 3064–3071, 2014.

[37] Y. Wu, P. Qiao, T. Chong, and Z. Shen, "Carbon Nanowalls Grown by Microwave Plasma Enhanced Chemical Vapor Deposition," *Advanced Materials*, vol. 14, no. 1, pp. 64–67, 2002.

[38] T. V. Cuong *et al.*, "Photoluminescence and Raman studies of graphene thin films prepared by reduction of graphene oxide," *Materials Letters*, vol. 64, no. 3, pp. 399–401, 2010.

[39] Y. Sakai, K. Takeda, and M. Hiramatsu, "Graphene growth in microwave-excited atmospheric pressure remote plasma enhanced chemical vapor deposition," *Japanese Journal of Applied Physics*, vol. 61, no. SA, p. SA1018, 2022.